Copyright WILEY-VCH Verlag GmbH & Co. KGaA, 69469 Weinheim, Germany, 2016.

Supporting Information

Synthetic Light-Curable Polymeric Materials Provide a Supportive Niche for Dental Pulp Stem Cells

Kyle H. Vining, Jacob C. Scherba, Alaina M. Bever, Morgan R. Alexander, Adam D. Celiz, and David J. Mooney**

Supplementary Experimental Methods –

Time-of-flight secondary-ion mass spectrometry (ToF-SIMS) analysis –

ToF-SIMS measurements were conducted using a ToF-SIMS 4 (IONTOF GmbH) instrument operated using a 25 kV Bi^{3+} primary ion source exhibiting a pulsed target current of ~1pA. Samples were scanned at a pixel density of 100 pixels per mm, with 8 shots per pixel over a given area. An ion dose of 2.45×10^{11} ions per cm^2 was applied to each sample area ensuring static conditions were maintained throughout. Both positive and negative secondary ion spectra were collected (mass resolution of >7000), over an acquisition period of 15 scans (the data from which were added together). Owing to the non-conductive nature of the samples, charge compensation was applied in the form of a low energy (20eV) electron floodgun.

Multivariate analysis - Principal component analysis (PCA) –

The ToF-SIMS spectral data were analyzed using principal component analysis (PCA) as previously described.[1] All positive and negative ion peak intensities in a ToF-SIMS spectrum were normalized to the total secondary ion counts to remove the influence of primary ion beam fluctuation. The positive and negative ion intensity data were arranged into one concatenated data matrix. PCA analysis was carried out using the Eigenvector PLS Toolbox 5.2. All datasets were mean-centered and square root mean scaled.

Atomic Force Microscopy (AFM) –

AFM of polymer samples was performed using a Dimension Icon FastScan instrument (Bruker) in PeakForce tapping quantitative nanomechanical mapping (QNM) mode using silicon nitride cantilevers. Force–indentation curves were fit using the DMT model with a pyramid indenter.

Preparation of primary human DPSCs and PDLFs –

DPSCs were acquired commercially from Lonza (Poietics human DPSCs, PT-5025) after 12 passages. According to the manufacturer, over 90% of cells tested positive for CD105, CD166, CD29, CD90, and CD73, and over 95% were negative for CD34, CD45, and CD133. The DPSCs were expanded in culture for 2 passages and then cryopreserved in complete growth media and 7.5% DMSO. DPSCs were thawed for subsequent experiments in aMEM (Gibco) complete media, containing 1% penicillin-streptomycin (P/S), 100 μM L-ascorbic acid, and 20% fetal bovine serum. Human periodontal ligament fibroplasts (PDLFs) were commercially obtained from extracted human teeth (Lonza, CC-7049) at passage 2 and cultured in stromal growth media (Lonza) for 2 additional passages prior to cryopreservation as previously described. Incubation conditions were 37C at 5% CO_2.

Quantitave polymerase chain reaction (qPCR) measurements –

RNA was isolated with PureLink RNA Micro Kit (Invitrogen), quantified by NanoDrop spectrophotometer, and cDNA was reverse-transcribed by iScript Advanced Reverse Transcription Supermix for RT-qPCR (Bio-Rad). Real-time quantitative PCR was performed using CFX96 or CFX394 (Bio-Rad) in duplicate with 10 ng of cDNA and 2x AdvancedSSO SYBR Green Supermix (Bio-Rad) in each reaction. Screening was performed to assess a wide range of genes associated with integrin signaling by using a Bio-Rad PrimePCR Integrin Outside-In Signaling H384 plate. Individual qPCR measurements were repeated on at least three replicate samples using Bio-Rad PrimePCR primers. Relative gene expression was

computed by the delta-delta Ct method, which compared Ct values to a control sample and reference gene (GAPDH). See Table S3 for list of individual gene primers.

Micro-computed tomography imaging (MicroCT)

MicroCT images were acquired at the Harvard Center for Nanoscale Systems with a tungsten filament in reflection mode (105 kV, 205 uA, 4 frames per projection). Following 3D reconstruction on VG studio, the coronal pulp in each tooth was segmented to calculate the mineralized volume of reparative dentin.

Supplementary Reference

[1] A. D. Celiz, J. G. W. Smith, A. K. Patel, R. Langer, D. G. Anderson, D. A. Barrett, L. E. Young, M. C. Davies, C. Denning, M. R. Alexander, *Biomaterials Science* **2014**, *2*, 1604.

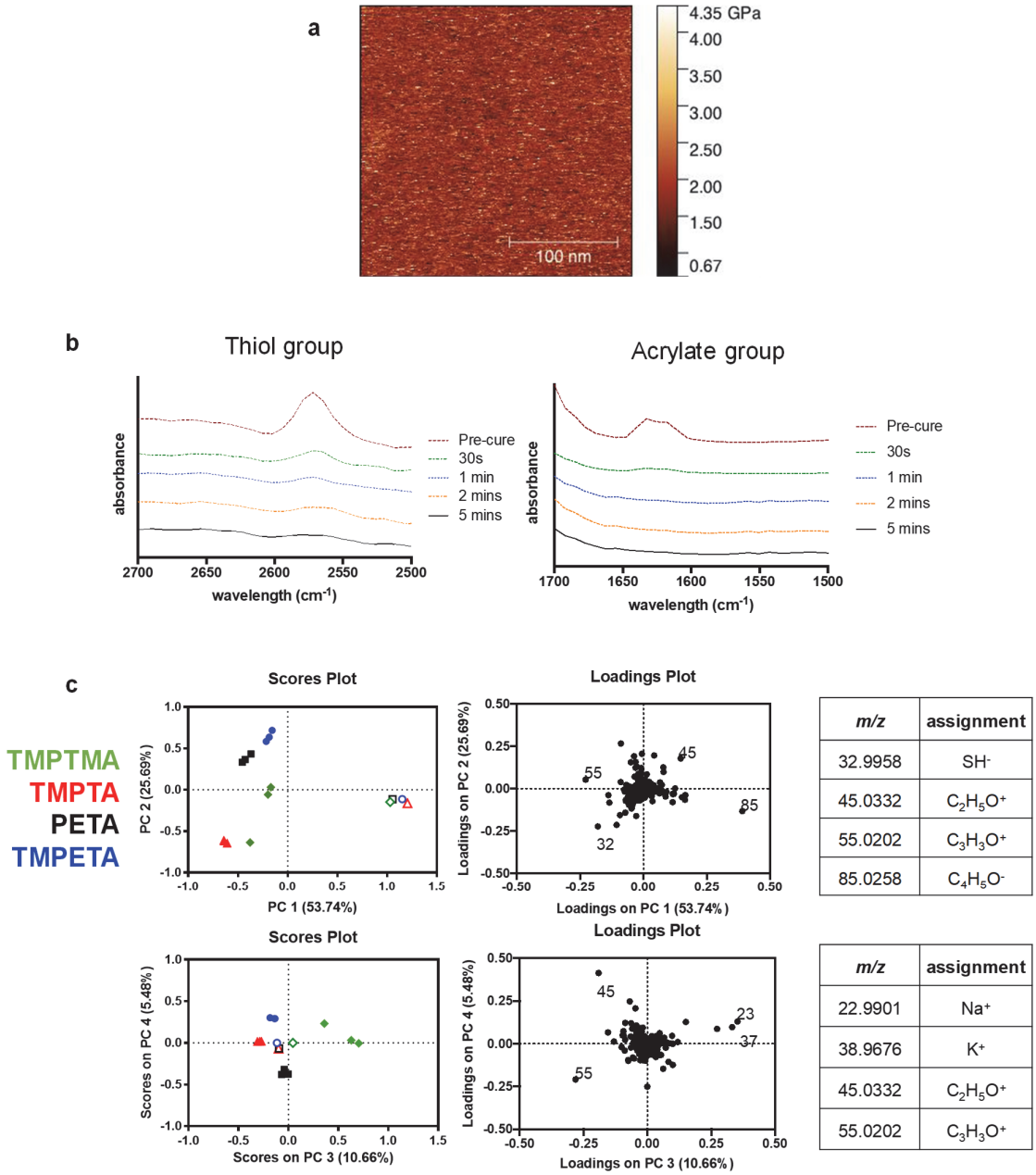

Figure S1. Physicochemical characterizations of thiol-ene-crosslinked triacrylate polymers. A) Representative spectrum of atomic force microscopy mechanical measurements of TMPTA, which showed high elastic moduli (~2 GPa) similar to TCP and dentin ~10 GPa, scale bar 100 nm. B) The residual acrylate and thiol chemical groups were measured on the surface of thiol-ene polymerized-TMPTA by Fourier-transform infrared spectroscopy, which showed significant attenuation of the acrylate and thiol peaks after curing. C) Comparison of the surface chemistry of arrayed (open symbols) and scaled-up polymers TMPTMA (green

diamond), TMPTA (red triangle), PETA (black square), and TMPETA (blue circle) was performed using principal component analysis (PCA) of the respective ToF-SIMS spectra. PCA revealed significant differences in surface chemistry between samples with principal component 1 represented the majority of chemical variance (53%) which was assigned to the substrate background poly(2-hydroxyethyl methacrylate) (pHEMA) moieties in the arrayed samples and thiol functionality present in the scaled-up polymers.

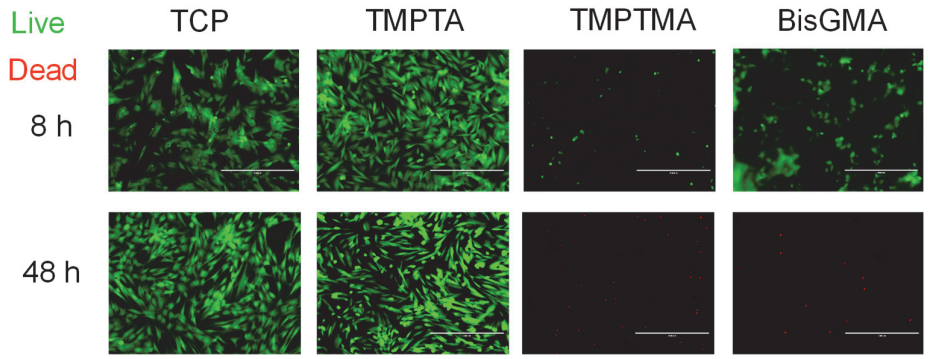

Figure S2. Live-dead staining at 8 and 48 hours showed that cells adhered to TMPTA exhibited similar viability as TCP, but significantly fewer viable cells were present on TMPTMA and BisGMA. Live – calcein (green), Dead – ethidium homodimer-1 (red). Scale bar 400 µm.

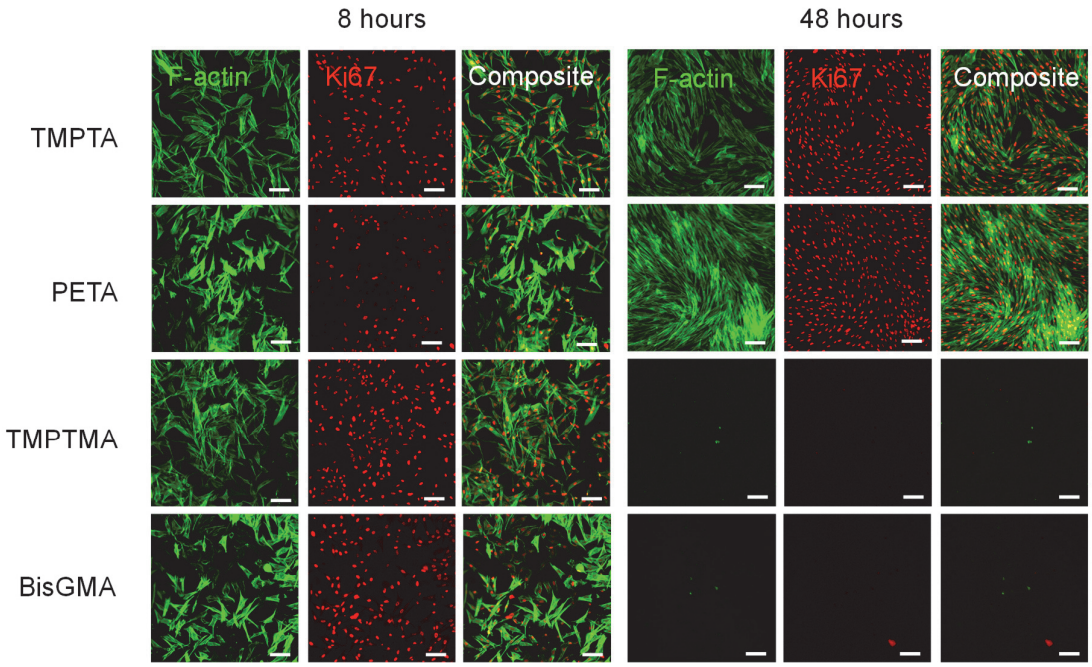

Figure S3. Confluent DPSCs under serum-free conditions express proliferation marker Ki67. Confocal microscopy of Ki67 immunostaining (red) and F-actin (green) at 8 and 48 hours on TMPTA, PETA, TMPTMA, and BisGMA, scale bar 100 µm.

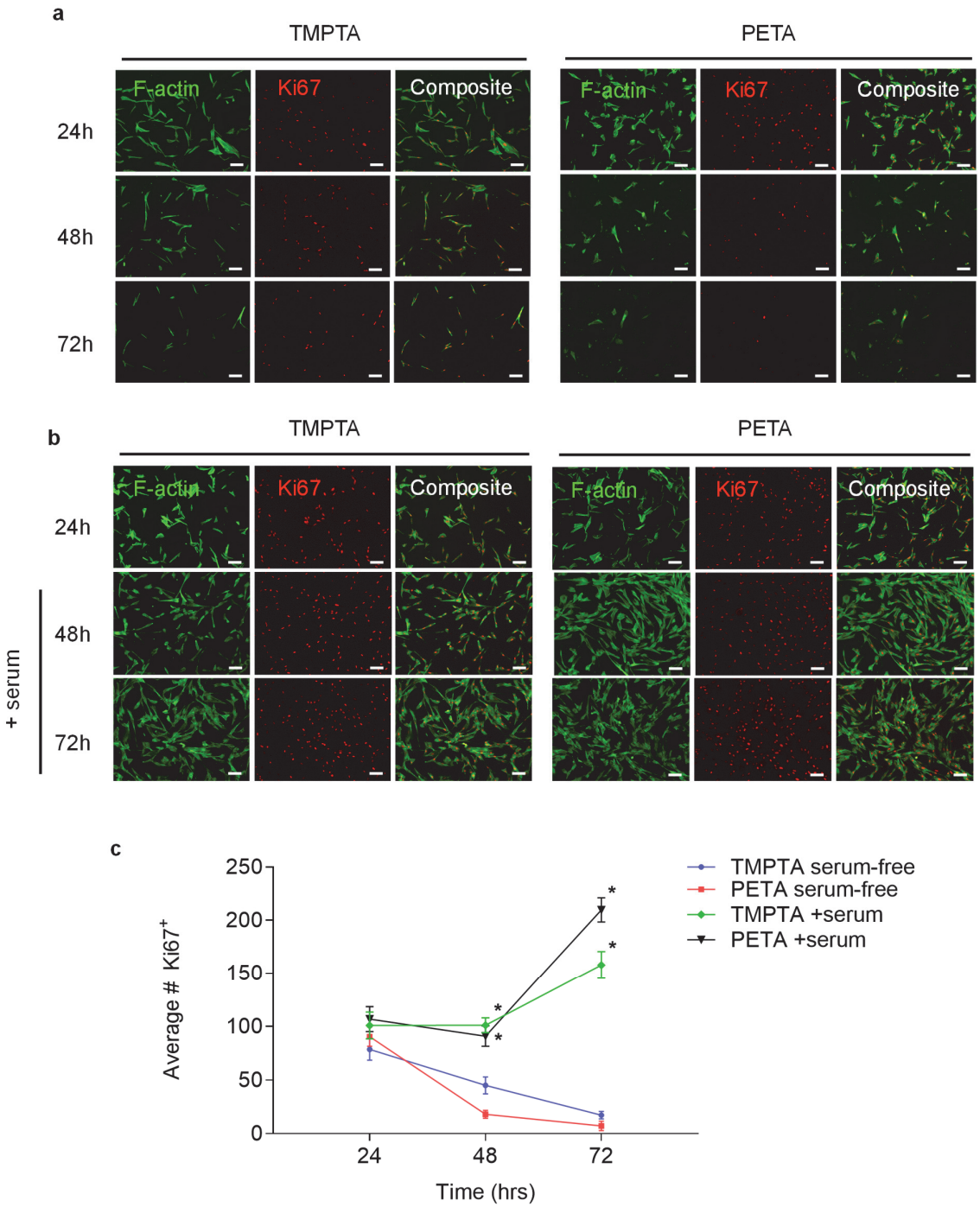

Figure S4. DPSCs maintain expression of proliferation marker Ki67 over 72 hours in serum-containing media. a) DPSCs seeded at subconfluent density (2.5 x10^4 cells/cm^2) on TMPTA and PETA in serum-free media show a reduction in Ki67 expression over 72 hours, as shown by fluorescence imaging of cells stained for F-actin (green) and Ki-67 (red). Scale bar 100 µm. b) DPSCs on TMPTA and PETA in serum-containing media continued to proliferate over 72

hours. DPSCs were adhered at low seeding density (2.5 x10^4 cells/cm^2) initially in serum-free media, which was replaced at 24 hours with media containing 10% FBS. Fluorescence imaging of Ki67 (red) and F-actin (green) staining show the growth and recovery of Ki67+ cells. Scale bar 100 µm. c) Quantification of average number of Ki67+ cells at 24, 48 and 72 hours on TMPTA and PETA, * statistically significant difference from TMPTA-serum free condition, $p<0.05$, $n \geq 8$.

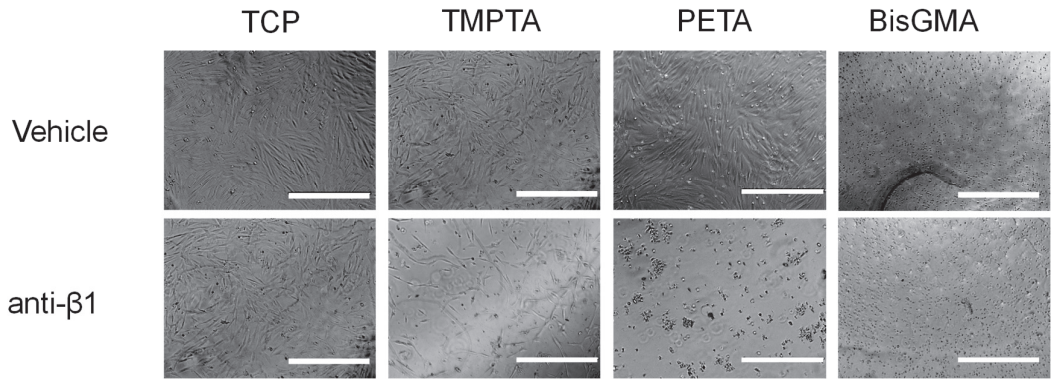

Figure S5. DPSCs adhere to and remain viable on triacrylates in an integrin-dependent manner. Phase images at 8 and 48 hours showed cells did not remain adhered on the triacrylates TMPTA and PETA, as well as BisGMA, when treated with an anti-β1 antibody to block the integrin β1 receptor subunit, while it had no significant effect on the tissue culture control TCP. Scale bar 400 µm.

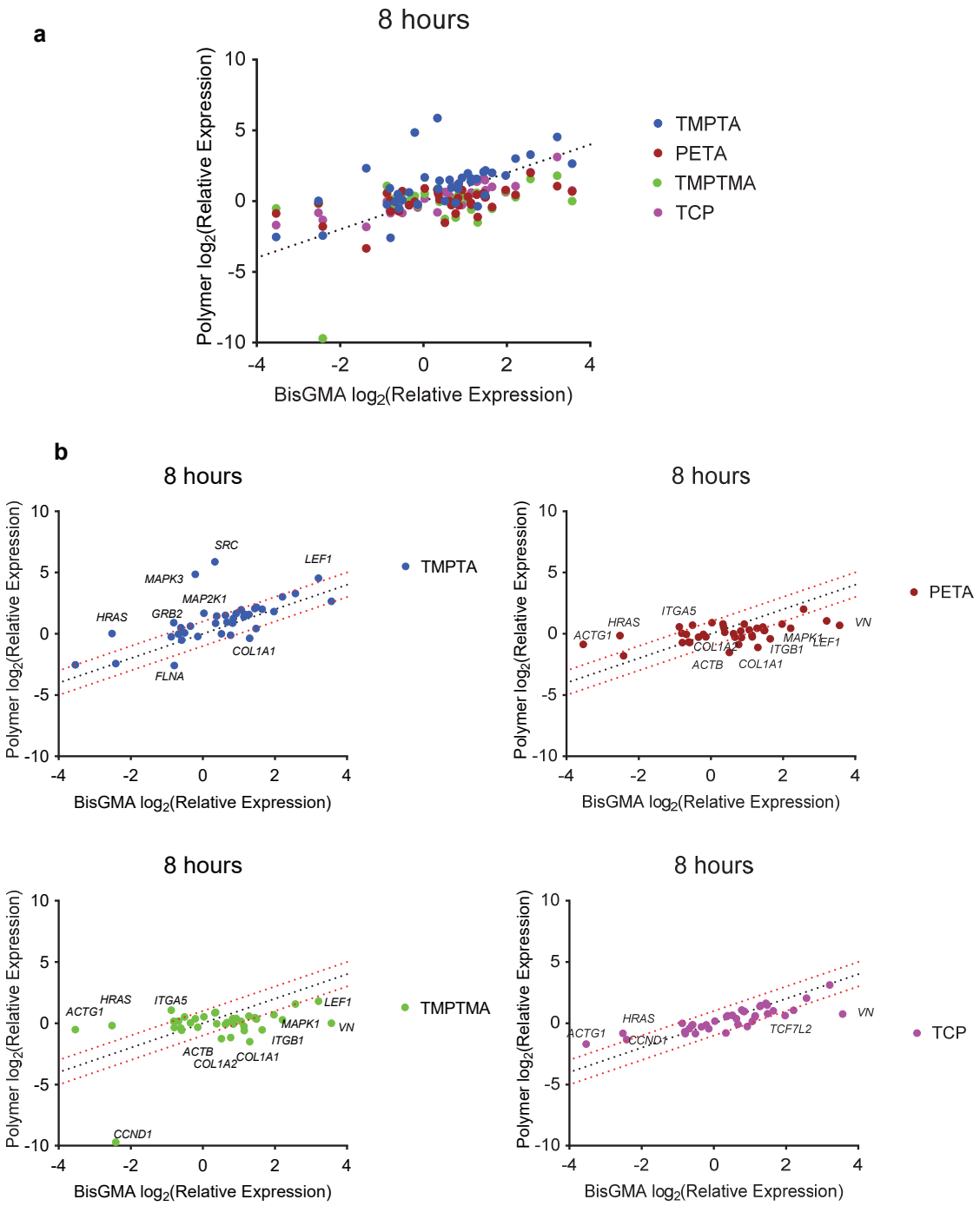

Figure S6. Gene expression analysis of DPSCs adhered after 8 hours to TCP, TMPTA, PETA, TMPTMA, TCP relative to BisGMA control. a) Differential expression of gene markers of β1 integrin signaling from a commercial gene array, using the BioRad PrimePCR Integrin Outside-In Signaling 384-well plate, normalized to GAPDH, n=2. Dotted line indicates unity

between polymer and BisGMA. b) Scatterplots used to identify differentially expressed genes (defined as above 2-fold threshold).

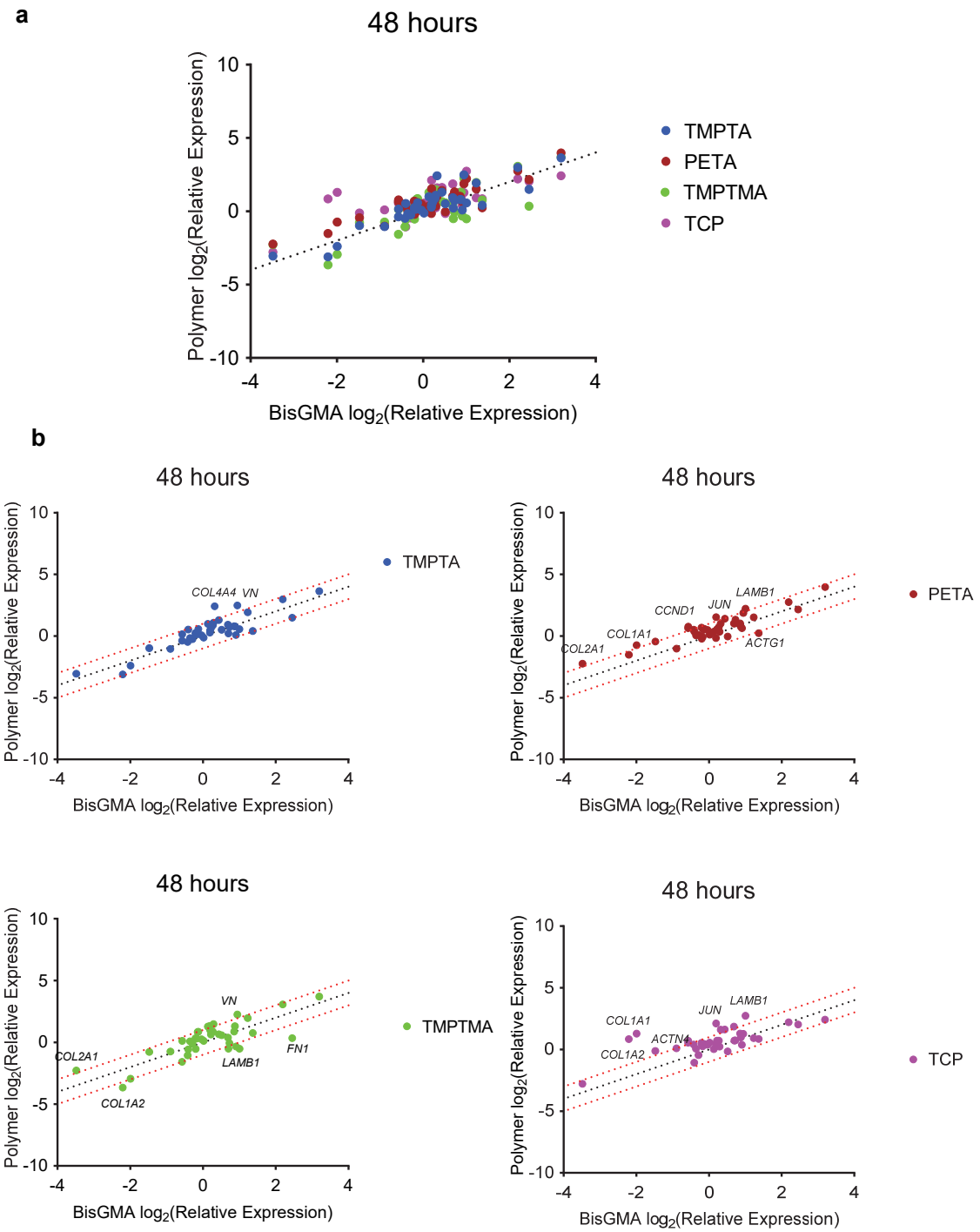

Figure S7. Gene expression analysis of DPSCs adhered after 48 hours to TCP, TMPTA, PETA, TMPTMA, and TCP relative to BisGMA control. a) Differential expression of gene

markers of β1 integrin signaling from a commercial gene array, using the BioRad PrimePCR Integrin Outside-In Signaling 384-well plate, normalized to GAPDH, n=2. Dotted line indicates unity between polymer and BisGMA. b) Scatterplots used to identify specific differentially expressed genes (defined as above 2-fold threshold).

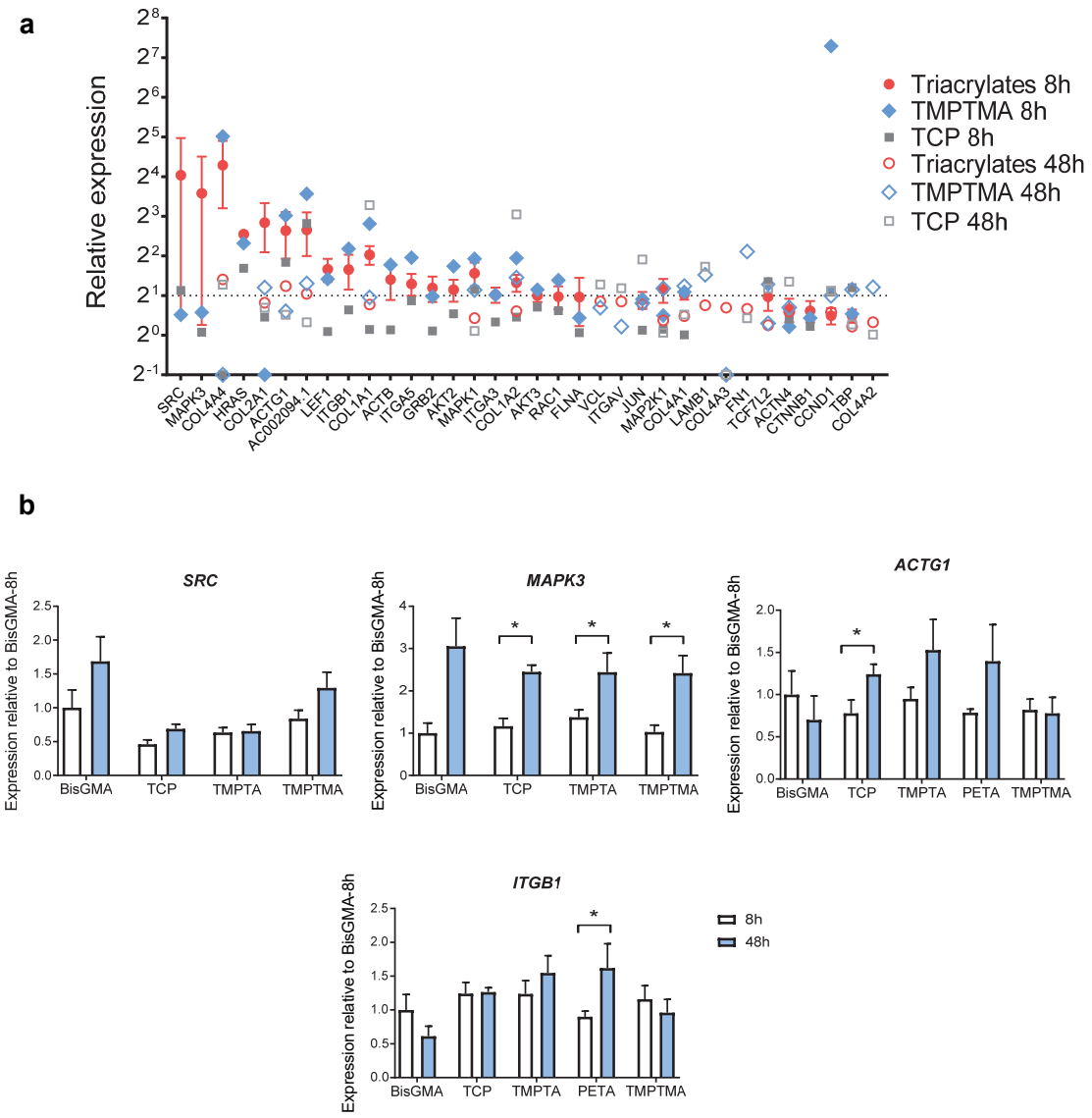

Figure S8. Candidate genes regulated by materials conditions. a) Ranked absolute relative gene expression of DPSCs adhered after 8 and 48 hours to TCP, triacrylates (mean of TMPTA and PETA), TMPTMA, and TCP, normalized to BisGMA control at 8 hours and GAPDH from the BioRad PrimePCR Integrin Outside-In Signaling gene array. b) Confirmation of

specific candidate genes by qPCR, in particular *SRC*, *MAPK3*, *ACTG1*, and *ITGB1* expression in DPSCs on BisGMA, TCP, TMPTA, PETA, and TMPTMA after 8 and 48 hours, normalized to BisGMA control at 8 hours and GAPDH, * statistically significant difference, two-way ANOVA, $p<0.05$, $n>3$.

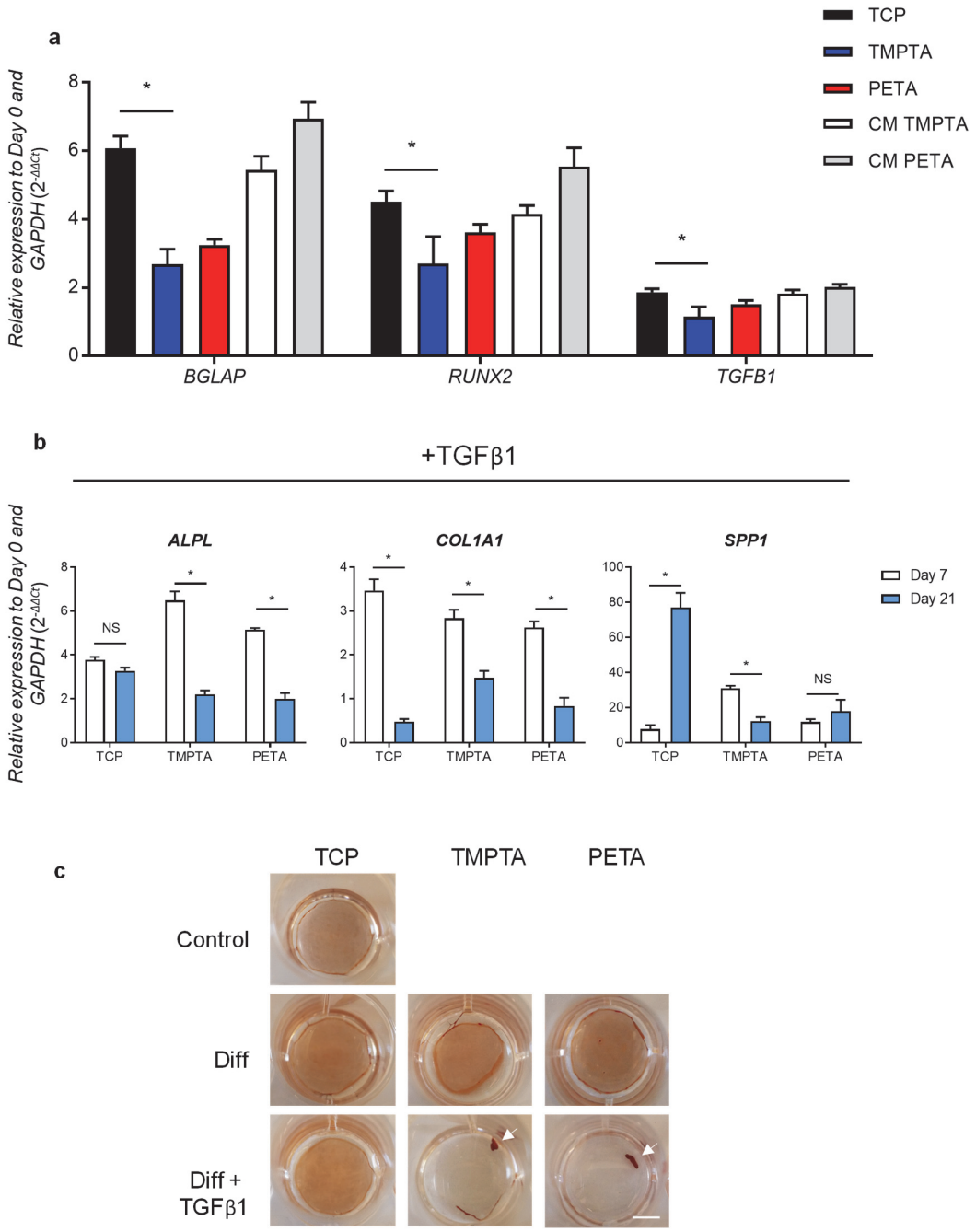

Figure S9. Gene expression of DPSCs on material conditions after long-term culture. a) Relative gene expression of osteocalcin (*BGLAP*), *RUNX2*, and *TGFB1* in DPSCs on TCP,

TMPTA and PETA after 21 days in serum-free media, as well as cells on TCP exposed to conditioned media from TMPTA and PETA (CM), * statistically significant difference, two-way ANOVA, $p<0.05$, $n > 3$. b) Relative expression of alkaline phosphatase (*ALPL*), collagen, type I (*COL1A1*), and osteopontin (*SPP1*) in DPSCs when cultured 7 and 21 days in osteogenic media with the addition of TGFβ1 on TCP, TMPTA, and PETA, normalized by GAPDH and Day 0, *statistically significant difference, two-way ANOVA, $p>0.05$, $n = 3$. c) Alizarin red staining of DPSCs on TCP, TMPTA, and PETA at 14 days under osteogenic conditions with (Diff + TGFβ1) or without (Diff) growth factor TGFβ1. DPSCs in TGFβ1-media contract into a cluster of cells on TMPTA and PETA (white arrow). Scale bar 5 mm.

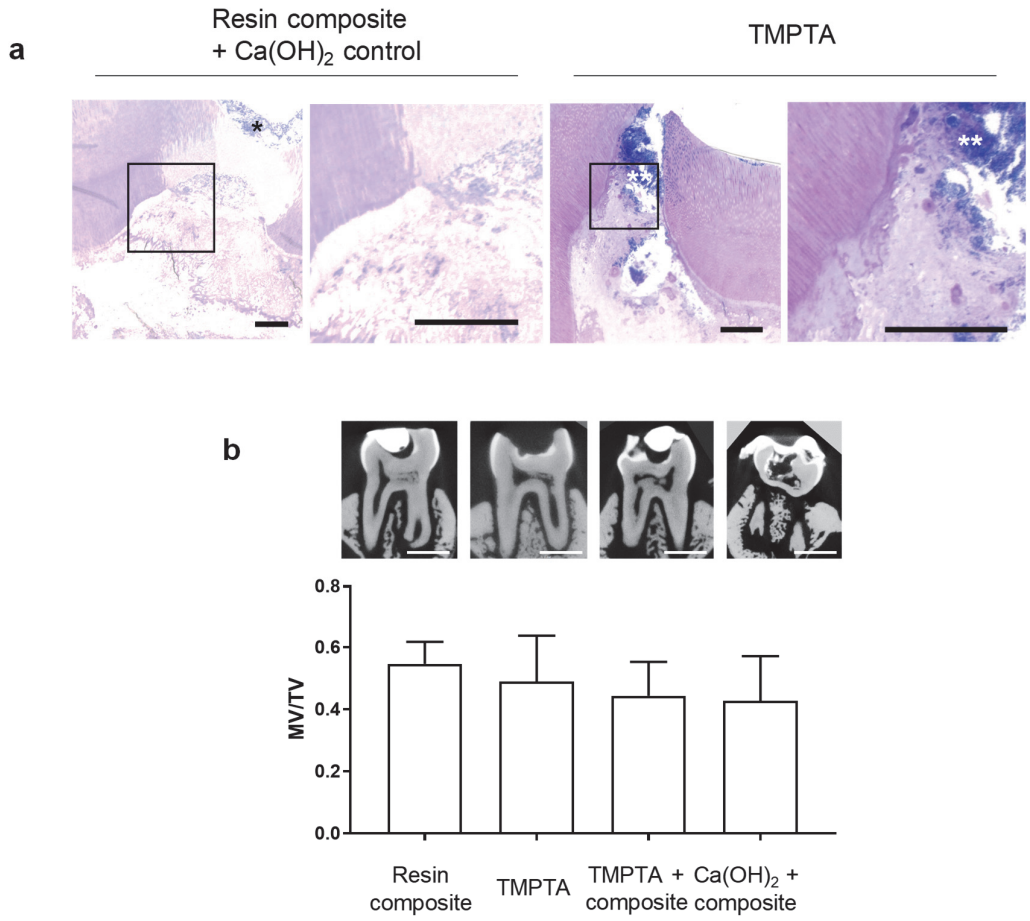

Figure S10. a) Hard tissue histological sections of TMPTA in direct contact with molar pulp defect at 8-weeks after injury (white asterisks), compared to control of calcium hydroxide paste and commercial dental resin composite (black asterisk). Scale bar 100 µm. b) MicroCT

analysis of dental pulp calcifications. MicroCT images and mineralized-volume to total-volume ratio, as measured at 8 weeks for treatment with commercially available dental resin composite, composite + calcium hydroxide paste, TMPTA, or TMPTA + commercial resin composite. Scale bar 1 mm. No statistically significant differences between groups, one-way ANOVA, $p>0.05$, $n = 2$.

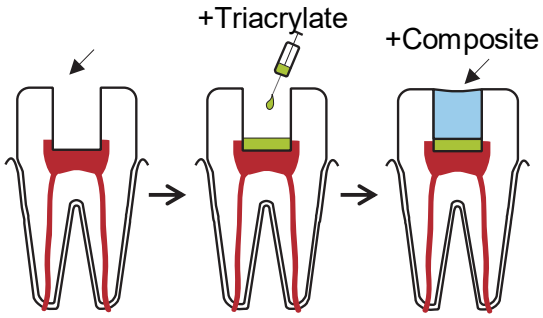

Figure S11. Proposed clinical application of triacrylate-based dental material to treat dental pulp injury following partial resection of pulp tissue (red) in molars and application of regenerative therapy (arrow). Triacrylate biomaterial (green) is placed in direct contact with treated pulp tissue to restore the dentin-pulp interface, because it supports DPSC regenerative behavior, and then is light-cured using traditional visible-light irradiation. Proper dental form and function are restored with a traditional dental composite material (blue). Alternatively, triacrylate-based materials could be used to develop one-step bio-instructive dental composite filling materials that are compatible with the dental pulp cells, as well as restore the tooth.

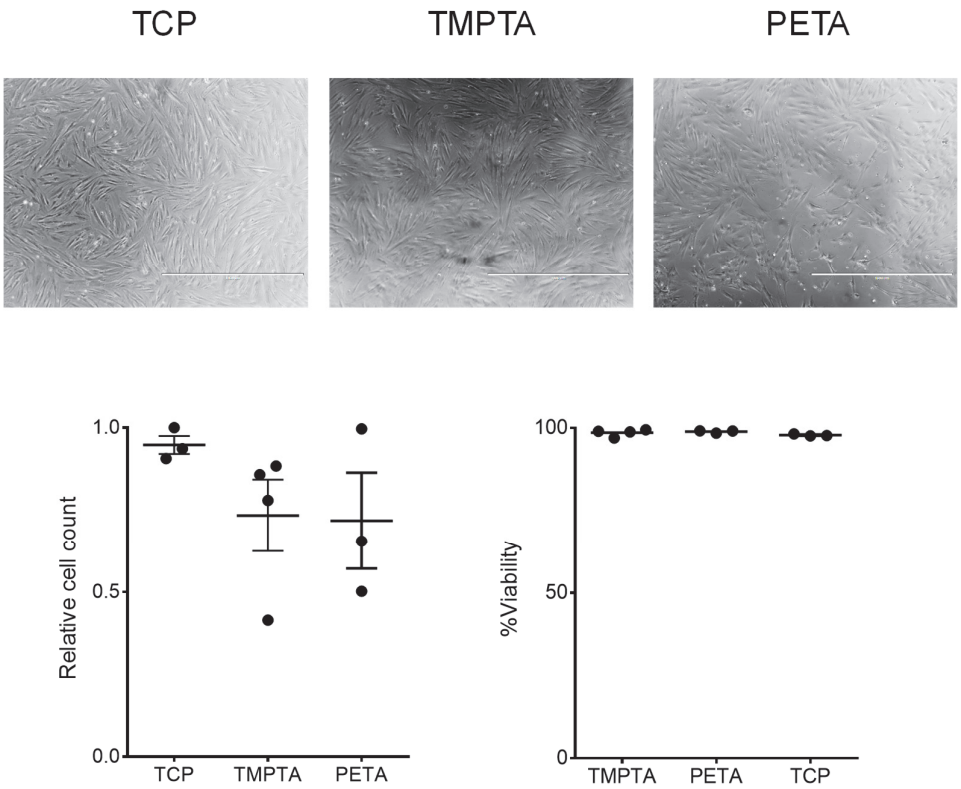

Figure S12. Triacrylate polymers TMPTA and PETA promoted adhesion of primary human periodontal ligament fibroblasts similar to tissue culture control (TCP). Phase images show confluent monolayers, scale bar 1 mm. Quantification of cell number, relative to highest cell number, and cell viability after 48 hours in serum-free media.

Table S1. Monomer list for polymer microarray

Monomer chemical name
Glycidyl methacrylate
N-(Butoxymethyl)acrylamide
N-Hydroxyethyl acrylamide
Benzyl 2-n-propyl acrylate
Norbornyl methacrylate
Isobornyl methacrylate
Methylthioethyl methacrylate
Caprolactone 2-(methacryloyloxy)ethyl ester
Hexadecafluoro-9-(trifluoromethyl)decyl acrylate
N-(Isobutoxymethyl)acrylamide

Tetrahydrofurfuryl acrylate
Hexafluoropent-1,5-diyl diacrylate
Tert-butylcyclohexylacrylate
Tricyclodecane-dimethanol diacrylate
Butanediol-1,3 diacrylate
Poly(ethylene glycol) methyl ether acrylate
N-[2-(1H-indol-3-yl)ethyl]acrylamide
N-[Tris(hydroxymethyl)methyl]acrylamide
N-(3-Methoxypropyl)acrylamide
Ter-butyl methacrylate
Stearyl methacrylate
Phenyl methacrylate
Isodecyl methacrylate
Acryloyloxy-β,β-dimethyl-γ-butyrolactone
Poly(ethylene glycol) phenyl ether acrylate
Hydroxypropyl acrylate
Dimethylamino-propyl acrylate
Isobutyl acrylate
Hydroxypivalyl hydroxypivalate bis[6-(acryloyloxy)hexanoate]
Tetra(ethylene glycol) diacrylate
Di(ethylene glycol) diacrylate
Acrylamide
N-Phenylmethacrylamide
Tri(ethylene glycol) methyl ether methacrylate
Glycerol dimethacrylate
Isobutyl methacrylate
Lauryl methacrylate
t-Butyl cyclohexyl methacrylate
Caprolactone 2-(methacryloyloxy)ethyl ester
Poly(propylene glycol) acrylate
Glycerol propoxylate triacrylate
Isodecyl acrylate
Isooctyl acrylate
Trimethylolpropane benzoate diacrylate
3-Hydroxy-2,2-dimethylpropyl 3-hyrdoxy-2,2-dimethylpropionate diacrylate
Ethylene glycol dimethacrylate
1,4-Bis(acryloyl)piperazine
N-(1,1,3,3-tetramethylbutyl)acrylamide
Hydroxybutyl methacrylate
Acryloyloxy-2-hydroxypropyl methacrylate
Decyl methacrylate
Ethylene glycol phenyl ether methacrylate
Diethylaminoethyl methacrylate
Ethylhexyl methacrylate

Pentaerythritol triacrylate
N-Methylmethacrylamide
Di(ethylene glycol) 2-ethylhexyl ether acrylate
Lauryl acrylate
Hexanediol ethoxylate diacrylate
Bisphenol A ethoxylate diacrylate
Dimethylamino-ethyl acrylate
N-(4-Hydroxyphenyl)methacrylamide
Methacrylamide
N-[3-(Dimethylamino)propyl]acrylamide
Vinyl methacrylate
Cyclohexyl methacrylate
Ethylene glycol methyl ether methacrylate
Ethylhexyl methacrylate
Tridecafluoro-2-hydroxynonyl acrylate
Poly(propylene glycol) methyl ether acrylate
Glycidyl acrylate
Benzyl acrylate
Epoxidized acrylate
Ethylene glycol diacrylate
Hexamethylene diacrylate
Neopentyl glycol diacrylate
N,N'-Ethylenebisacrylamide
Sulfopropyl acrylate potassium salt
Di(ethylene glycol) methyl ether methacrylate
Butyl methacrylate
Tetrahydrofurfuryl methacrylate
Poly(ethylene glycol) methyl ether methacrylate
Poly(ethylene glycol) methacrylate
Hexyl methacrylate
Hydroxy-3-phenoxypropyl acrylate
Hydroxy-3-phenoxypropyl acrylate
Di(ethylene glycol) ethyl ether acrylate
Hexyl acrylate
Glycerol 1,3-diglycerolate diacrylate
Neopentyl glycol propoxylate diacrylate
Ethylene glycol methyl ether acrylate
Diacetone acrylamide
N-(Hydroxymethyl)acrylamide
Butoxyethyl methacrylate
tetraethyleneglycol dimethacrylate
Furfuryl methacrylate
Tert-butylamino-ethyl methacrylate
Ethylene glycol dicyclopentenenyl ether methacrylate

Tri(ethylene glycol) dimethacrylate
Butylamino carbonyl oxy ethyl acrylate
Trimethylolpropane ethoxylate triacrylate
Poly(propylene glycol) 4-nonylphenyl ether acrylate
Trimethylhexyl acrylate
Poly(propylene glycol) diacrylate
Trimethylolpropane ethoxylate methyl ether diacrylate
[2-(Methacryloyloxy)ethyl]dimethyl-(3-sulfopropyl) ammonium hydroxide
N-tert-Butylacrylamide
mono-2-(Methacryloyloxy)ethyl succinate
N-[3-(Dimethylamino)propyl]methacrylamide
Methyl 3-hydroxy-2-methylenebutyrate
Methacryloyloxy)ethyl acetoacetate
Benzyl methacrylate
Ethyl-cis-B-cyano-acrylate
Hydroxybutyl acrylate
Trimethylolpropane propoxylate triacrylate
Isobornyl acrylate
Propargyl acrylate
Butanediol diacrylate
Methyl-1,2-ethanediyl bis[oxy(methyl-2,1-ethanediyl)]diacrylate

Table S2. BioRad PrimePCR_Integrin Outside-In Signaling H384 Plate

Gene	Gene Name	PrimePCR ID
ACTB	actin, beta	qHsaCED0036269
ACTG1	actin, gamma 1	qHsaCED0005010
ACTN1	actinin, alpha 1	qHsaCED0002731
ACTN4	actinin, alpha 4	qHsaCID0012278
CTNNB1	catenin (cadherin-associated protein), beta 1, 88kDa	qHsaCID0010363
COL1A1	collagen, type I, alpha 1	qHsaCED0002181
COL1A2	collagen, type I, alpha 2	qHsaCED0003988
COL2A1	collagen, type II, alpha 1	qHsaCED0001057
COL4A1	collagen, type IV, alpha 1	qHsaCID0010223
COL4A2	collagen, type IV, alpha 2	qHsaCED0004426
COL4A3	collagen, type IV, alpha 3 (Goodpasture antigen)	qHsaCID0013308
COL4A4	collagen, type IV, alpha 4	qHsaCID0016411
CCND1	cyclin D1	qHsaCID0013833
FN1	fibronectin 1	qHsaCID0012349
FLNA	filamin A, alpha	qHsaCID0010844
GAPDH	glyceraldehyde-3-phosphate dehydrogenase	qHsaCED0038674
GSK3B	glycogen synthase kinase 3 beta	qHsaCID0010097
GRB2	growth factor receptor-bound protein 2	qHsaCED0004795
HPRT1	hypoxanthine phosphoribosyltransferase 1	qHsaCID0016375
ITGA2	integrin, alpha 2	qHsaCID0016134
ITGA3	integrin, alpha 3	qHsaCID0010823
ITGA5	integrin, alpha 5	qHsaCID0021495
ITGAV	integrin, alpha V	qHsaCID0006233
ITGB1	integrin, beta 1	qHsaCED0005248
ILK	integrin-linked kinase	qHsaCED0038739
JUN	jun proto-oncogene	qHsaCED0018770
LAMB1	laminin, beta 1	qHsaCID0006489

LEF1	lymphoid enhancer-binding factor 1	qHsaCED0001977
MAPK1	mitogen-activated protein kinase 1	qHsaCID0006818
MAPK3	mitogen-activated protein kinase 3	qHsaCID0010939
MAP2K1	mitogen-activated protein kinase kinase 1	qHsaCID0011553
gDNA	PrimePCR DNA Contamination Control Assay	qHsaCtlD0001004
PCR	PrimePCR Positive Control Assay	qHsaCtlD0001003
RT	PrimePCR Reverse Transcription Control Assay	qHsaCtlD0001001
RQ1	PrimePCR RNA Quality Assay	qHsaCtlD0001002
RQ2	PrimePCR RNA Quality Assay	qHsaCtlD0001002
PTK2	PTK2 protein tyrosine kinase 2	qHsaCED0001879
RAC1	ras-related C3 botulinum toxin substrate 1 (rho family, small GTP binding protein Rac1)	qHsaCED0001330
TBP	TATA box binding protein	qHsaCID0007122
TCF7L2	transcription factor 7-like 2 (T-cell specific, HMG-box)	qHsaCID0012510
AKT1	v-akt murine thymoma viral oncogene homolog 1	qHsaCID0011338
AKT2	v-akt murine thymoma viral oncogene homolog 2	qHsaCED0037964
AKT3	v-akt murine thymoma viral oncogene homolog 3	qHsaCID0036448
HRAS	v-Ha-ras Harvey rat sarcoma viral oncogene homolog	qHsaCED0023908
VCL	vinculin	qHsaCID0020885
AC002094.1	Vitronectin	qHsaCED0001902
RAF1	v-raf-1 murine leukemia viral oncogene homolog 1	qHsaCED0001147
SRC	v-src sarcoma viral oncogene homolog (avian)	qHsaCED0004489

Table S3. BioRad PrimePCR assays for qPCR

Gene	Gene Name	PrimePCR ID
AC002094.1 (VN)	Vitronectin	qHsaCED0001902
ACTA2	Smooth muscle actin	qHsaCID0013300
ACTG1	Actin, gamma 1	qHsaCED0005010
ALPL	Alkaline phosphatase	qHsaCED0045991
BGLAP	Osteocalcin	qHsaCED0038437
CCND1	Cyclin D1	qHsaCID0013833
COL1A1	Collagen, type I, alpha 1	qHsaCED0043248
COL2A1	Collagen, type II, alpha 1	qHsaCED0001057
COL4A4	Collagen, type IV, alpha 4	qHsaCID0016411
DSPP	Dentin sialophosphoprotein	qHsaCED0002962
GAPDH	Glyceraldehyde-3-phosphate dehydrogenase	qHsaCED0038674
HRAS	Harvey rat sarcoma viral oncogene homolog	qHsaCED0023908
ITGB1	integrin, beta 1	qHsaCED0005248
LEF1	Lymphoid enhancer-binding factor 1	qHsaCED0001977
MAPK3	Mitogen-activated protein kinase 3	qHsaCID0010939
RUNX2	Runx-2	qHsaCED0044067
SPP1	Secreted phosphoprotein 1, osteopontin	qHsaCED0057074
STC1	Staniocalcin	qHsaCID0006115
SRC	v-src sarcoma viral oncogene homolog (avian)	qHsaCED0004489